International Journal of Pharmaceutics, 3 (1979) 261–274

DISSOLUTION ANISOTROPY IN NICKEL SULFATE α HEXAHYDRATE CRYSTALS

HELEN M. BURT and A.G. MITCHELL *

Faculty of Pharmaceutical Sciences, University of British Columbia, Vancouver, B.C. V6T 1W5 (Canada)

(Received February 3rd, 1979)
(Revision version received March 19th, 1979)
(Accepted March 26th, 1979)

SUMMARY

The dissolution anisotropy of well-formed crystals of $NiSO_4$ α $6H_2O$ grown under controlled conditions was studied using a single crystal dissolution method. Dissolution rates, proportional to an observed apparent rate constant, K_{obs}, were determined by measuring the movement of the (111) and (112) crystal faces with time in a flowing solvent, using a travelling microscope. K_{obs} for the (112) face was greater than for the (111) face at all flow rates studied but anisotropy was less pronounced at the lower flow rates. The apparent rate constants for the transport and surface controlled reactions, K_t and K_r, were of the same order of magnitude suggesting that the overall dissolution reaction was under mixed control at the lower flow rates. Activation energies were slightly higher than the normal range for transport processes. $K_r(112) > K_r(111)$ indicating that anisotropy was due mainly to differences in the rate of the surface reaction. At high flow rates there was a change to a predominantly surface controlled reaction and activation energies were within the accepted limits for these reactions. It is likely that dissolution anisotropy is due to the differences in activation energy for the two faces.

INTRODUCTION

The crystalline characteristics of a solid, e.g. its polymorphic form (Milosovich, 1964), degree of solvation (Shefter and Higuchi, 1963) and degree of crystallinity (Florence and Salole, 1976), may exert a significant effect on its dissolution rate. In addition, it is generally accepted that the various crystal faces, planes, or axes of anisotropic crystals may dissolve at different rates (Roller, 1932; Bunn, 1961).

Application of the kinetic theories of heterogeneous reactions (Van Name and Hill,

* To whom enquiries should be addressed.

1916; Bircumshaw and Riddiford, 1952) to this phenomenon of dissolution anisotropy suggest three possibilities:

(1) The rate of the reaction at the crystal–solvent interface is very much faster than the rate of transport of products from the surface. Dissolution is therefore determined solely by the rate of the slower transport process, i.e. transport controlled dissolution. Under the same hydrodynamic conditions the rate should be the same for each face of both isotropic and anisotropic crystals.

(2) The rate of the surface reaction is much slower than the rate of the transport process and is therefore rate controlling, i.e. surface-controlled dissolution. The variation of properties with crystallographic direction is characteristic of all crystals, except those belonging to the isometric system, and results in a difference in surface free energy between faces with different Miller indices. Hence where dissolution is controlled by the rate of the surface reaction, unlike faces of anisotropic crystals should dissolve at different rates.

(3) When both rates are of the same order of magnitude the observed rate is a function of the two and the reaction is said to be of the intermediate type, i.e. mixed transport–surface-controlled dissolution. Transport-controlled and surface-controlled dissolution processes are limiting cases of the intermediate type and the distinction between the three possibilities will not be sharp.

Although dissolution anisotropy is a fundamental property of all non-isometric crystals, this aspect of dissolution has received little attention. Indeed Mullin (1972) has stated 'different crystallographic faces may grow at different rates, they may even dissolve at different rates but reliable measurements of this behavior have not been reported'. Although perhaps an overstatement, a literature search has revealed few papers comparing the dissolution rates of different crystal faces (Treivus, 1964; Karshin and Grigoryan, 1970; Ravdel and Moshkevich, 1971; Haussuhl and Muller, 1972; Cornell et al., 1974). The overall conclusion from these papers is that whether dissolution anisotropy is observed or not, depends on the experimental conditions. By changing variables such as degree of agitation, temperature or dissolution medium, either a transport-controlled or a surface-controlled or a mixed-controlled dissolution may be obtained.

Transport-controlled dissolution is generally represented by the Noyes–Nernst model in which it is assumed that a saturated layer of solute is established almost instantaneously at the solid–solvent interface. Mass transport of solute molecules and therefore dissolution rate, is determined entirely by Brownian movement diffusion through a stationary liquid film of thickness h, adhering to the solid surface and is given by

$$\text{rate} = S\, k_t(C_s - C) \qquad (1)$$

where k_t, the transport rate constant, =D/h and D is the diffusion coefficient in the saturated layer, C_s is the equilibrium concentration in the saturated layer, C is the concentration in the bulk solution at time t, and S is the surface area of the solid.

The Noyes–Nernst equation has been extended to include reactions of the interme-

diate type (Wurster and Taylor, 1965a, b; Nogami et al., 1969; Donbrow and Touitou, 1977) in which it is assumed that the surface and transport processes occur in consecutive steps and the overall rate is given by

$$\text{rate} = S\, k_{obs}(C_s - C) \tag{2}$$

where k_{obs} is the observed rate constant for mixed controlled dissolution and is equal to

$$k_{obs} = \frac{k_r k_t}{k_r + k_t} \tag{3}$$

where k_r is the rate constant for the surface-controlled reaction. When $k_r >> k_t$ the overall rate is determined solely by the transport process and Eqn. 2 becomes the Noyes–Nernst equation. The condition $k_t >> k_r$ represents the case of surface-controlled dissolution in which the concentration in the interfacial layer, C_i, is less than the equilibrium solubility (Van Name and Hill, 1916). Berthough (1912) suggested that the different crystallization rates of the various crystal faces was due to differences in k_r. It seems likely that the variation in dissolution rates between faces with different Miller indices may be explained in a similar manner.

In a transport-controlled process, h for laminar flow over a flat plate is given by Eqn. 4 (Levich, 1962).

$$h = 3x^{1/2}D^{1/3}v^{1/6}u^{-1/2} \tag{4}$$

where x is the distance from the upstream edge of the plate measured along an axis parallel to the direction of flow, v is the kinematic viscosity of the solvent, and u is the linear flow rate. Rearrangement of Eqn. 4 and substitution for h gives

$$k_t = 0.33x^{-1/2}D^{2/3}v^{-1/6}u^{1/2} \tag{5}$$

For a mixed-controlled dissolution reaction the individual rate constants k_t and k_r can be obtained by rearranging Eqn. 3

$$\frac{1}{k_{obs}} = \frac{1}{k_t} + \frac{1}{k_r} \tag{6}$$

and substituting for k_t from Eqn. 5

$$\frac{1}{k_{obs}} = 3x^{1/2}D^{-2/3}v^{1/6}u^{-1/2} + \frac{1}{k_r} \tag{7}$$

Hence by plotting k_{obs}^{-1} against $u^{-1/2}$ it is possible to calculate k_t at each flow rate from (1/slope) $u^{1/2}$ and k_r from 1/intercept.

MATERIALS AND METHODS

Materials

Nickel sulfate ($NiSO_4 \alpha 6H_2O$) grows as a well-formed crystal, its shape being a combination of two tetragonal bipyramids, and is an ideal model for single crystal studies. The crystals were grown in a fluidized bed crystallizer under carefully controlled conditions. Details of the conditions of crystal growth have been reported previously (Phillips and Epstein, 1974). Crystals selected for the dissolution studies were between 4.0 and 4.8 mm in width and 4.5 and 5.0 mm in length with well-defined crystalline faces (Fig. 1). The dissolution solvent was 60% ethanol prepared by diluting 95% ethanol (commercial grade) with distilled water.

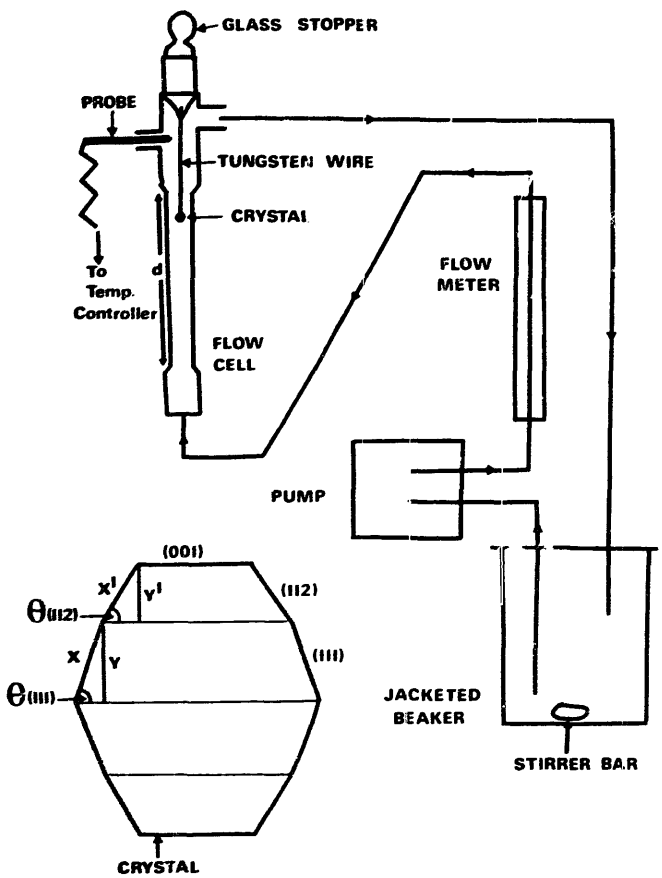

Fig. 1. Dissolution apparatus and diagram of a single $NiSO_4 \alpha 6H_2O$ crystal showing geometry and position of crystal faces, characterized by their Miller indices.

Dissolution measurements

Apparatus

The dissolution flow cell (Fig. 1) was designed by Mullin and Garside (1967) to measure the growth rates of individual crystal faces. The solvent reservoir was a 600 ml jacketed glass beaker connected to a constant temperature circulator (Haake FT) and fitted with a cover to minimize solvent evaporation. Ethanol in the jacketed beaker was stirred using a magnetic stirrer and a 3.5 cm Teflon-coated stirrer bar. The solvent was drawn from the beaker by a variable speed peristaltic pump (Manostat, Varistaltic, advanced model) fitted with silastic 1 cm internal diameter tubing, through a calibrated glass flow meter (Gilmont, size 4 flowmeter, range 10–850 ml · min^{-1}) into the flow cell back to the beaker. The distance, d, of the flow cell was 10.5 cm with an internal diameter of 1.5 cm. The required temperature in the cell was maintained by heating tape wound around the lower half of the cell and was monitored initially by a thermometer placed in the top. The temperature was controlled to ±0.05°C using a stainless steel probe (YSI series 400) and a temperature controller (Thermistemp model 71A) connected through a variable autotransformer to the heating tape.

Measurement

The (001) face of the crystal was fixed using one drop of cyanoacrylate glue (Krazy Glue) to a tungsten wire, 1 mm diameter and 8 cm length, sealed into a ground glass stopper. When temperature and flow rate had been stabilized at the desired conditions, the thermometer was removed and replaced by the glass stopper carrying the crystal. The movement of the (111) or (112) crystal face was measured with a travelling microscope (Swift and Son) reading to ±0.0005 cm. The observer's head was positioned in a head rest attachment from a gonioscope to prevent parallax errors. Dissolution was followed at flow rates of between 100 and 800 ml · min^{-1} at temperatures of 30, 37, 41 and 45.5°C for 50–60 min during which time there was negligible change in surface area. Dissolution occurred under sink conditions since at no time did the concentration of nickel sulfate exceed 1.5% of its saturation solubility. The experimental flow rates (cm^3 s^{-1}) were converted to linear flow rates, u, (cm s^{-1}) by dividing by the cross-sectional area (cm^2) of the flow cell and correspond to Reynolds numbers of between 100 and 800 which is in the range of laminar flow.

Correction factors

The travelling microscope measured the movement of the observed crystal face in a vertical direction, i.e. distance a in Fig. 2, whereas b, the movement in a direction perpendicular to the face was required. Hence all readings were corrected according to Eqn. 8.

$$b = a \cos \theta \tag{8}$$

where the values of θ, obtained from the geometry of the crystal (Fig. 1) were 70°54′ and 59°16′ for the (111) and (112) faces respectively (Phillips and Epstein, 1974).

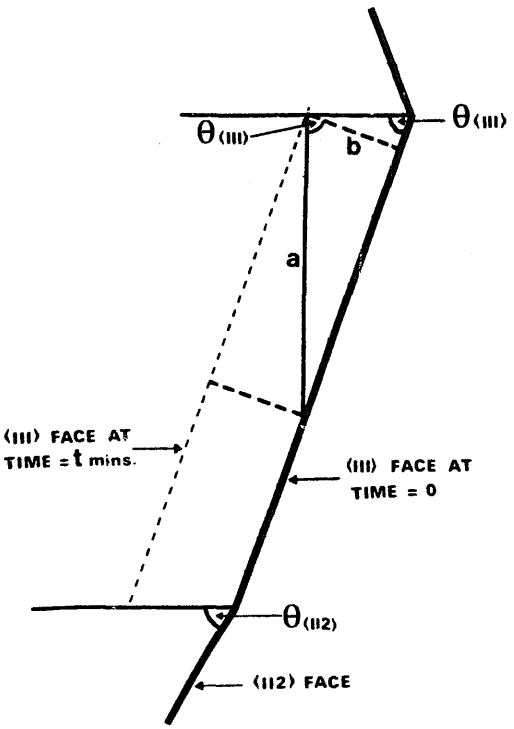

Fig. 2. Correction factors for the (111) and (1$\bar{1}$2) faces of $NiSO_4 \alpha 6H_2O$.

Physicochemical constants

Length of crystal face

The flat plates defined in Eqn. 4 were assumed to be the lengths of the (111) and (112) faces as presented to the direction of flow and are designated x and x^1 respectively. The lengths y and y^1 (Fig. 1) were measured with the travelling microscope and x and x^1 (Table 1) calculated from

$$x = y/\sin\theta \tag{9}$$

Kinematic viscosity

The kinematic viscosity of the dissolution medium, v, is given by η/ρ where η and ρ are the viscosity and density of 60% ethanol, respectively. Literature values of η and ρ were obtained at different temperatures (International Critical Tables, 1928; Lange, 1967), the values at 37° and 41°C being interpolated from plots of η and ρ versus temperature (Table 1).

TABLE 1

PHYSICAL CONSTANTS OF 60% ETHANOL AND $NiSO_4 \alpha 6H_2O$

Temperature (°C)	$\eta \times 10^2$ ($g \cdot cm^{-1} \cdot s^{-1}$)	p ($g \cdot cm^{-3}$)	$v \times 10^2$ ($cm^2 \cdot s^{-1}$)	$D \times 10^6$ ($cm^2 \cdot s^{-1}$)	x (111) face (cm)	x^1 (112) face (cm)
37	1.56	0.886	1.76	3.88	0.135 [a]	0.114 [a]
41	1.40	0.883	1.59	3.82	(0.109–0.159) [b]	(0.111–0.118) [b]

[a] Mean of 6 crystals.
[b] Range.

Diffusion coefficient

The diffusion coefficient, D, of $NiSO_4 \alpha 6H_2O$ was calculated from the Stokes–Einstein equation (Carstensen, 1977)

$$D = \frac{R}{L} \cdot \frac{T}{6\pi\lambda\eta} \tag{10}$$

where R/L is Boltzmann's constant (1.38×10^{-16} erg · deg^{-1}), T is absolute temperature and λ is the molecular radius. It was assumed that the diffusing species were the hydrated, complex ion $[Ni(6H_2O)]^{2+}_{aq.}$ and the hydrated sulfate ion, $SO_4^{2-}{}_{aq.}$ Hydrated (and complex) ions may be regarded as charged spheres the radius of which is the sum of the ionic radius and the diameter of the water molecule (2.76 Å) (George and McClure, 1959), giving ionic radii of 3.54 Å and 5.06 Å for $[Ni(6H_2O)]^{2+}_{aq.}$ and $SO_4^{2-}{}_{aq.}$ respectively. It was also assumed that the effect of water–ethanol interactions and of temperature change on the radius of the hydrated ions will be small and will not significantly affect the calculated values of the ionic radii. Substitution of the constants into Eqn. 10 gives, at 37°C,

$$D[Ni(6H_2O)]^{2+}_{aq.} = Dc = 4.11 \times 10^{-6} \text{ cm}^2 \cdot \text{sec}^{-1}$$

and

$$D\,SO_4^{2-}{}_{aq.} = D_a = 2.87 \times 10^{-6} \text{ cm}^2 \cdot \text{sec}^{-1}$$

An average value, D_{av}, for the cation D_c and the anion D_a was obtained from an equation derived by Nernst (Moore, 1972)

$$D_{av} = \frac{2 D_c D_a}{D_c + D_a} \tag{11}$$

D_{av} at 41°C was calculated by the same method (Table 1).

RESULTS AND DISCUSSION

When $C_s \gg C$ and S is constant, the overall dissolution rate is proportional to k_{obs} (Eqn. 2). Fig. 3 shows typical plots of distance moved as a function of time for a crystal face. The slopes, (cm · s^{-1}), determined using linear regression analysis [1], are proportional to the dissolution rate (g · cm^{-3} · s^{-1}) and were used as a measure of an observed apparent rate constant, K_{obs}.

An initial surge in the movement of the movement of the face was often observed between t = 0–10 min, and the slope was therefore calculated from the linear proportion of the curve after t = 10 min. On repeating an experiment on the same crystal under identical conditions the initial surge was not observed and the rate was equal to that of

[1] Using a Wang 600 programmable calculator.

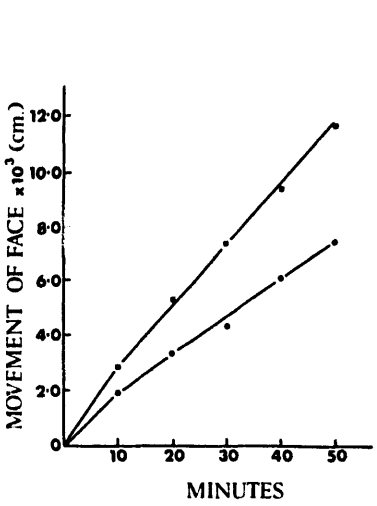

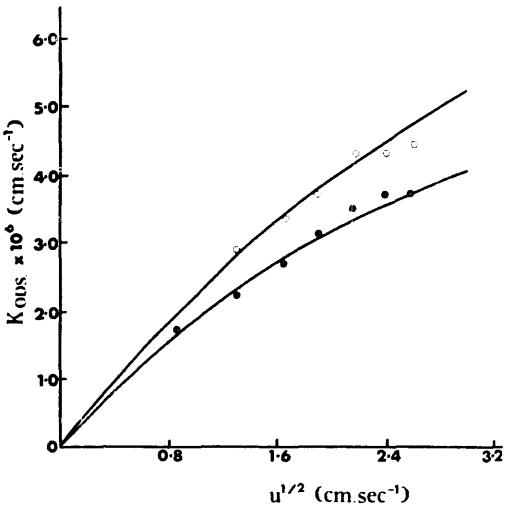

Fig. 3. Movement of the (111) crystal face as a function of time at 37°C. Flow rates: •, 1.70 cm · s^{-1}; ▪, 6.9 cm · s^{-1}.

Fig. 4. Dissolution anisotropy of $NiSO_4$ α $6H_2O$ at 37°C: •, (111) face; ○ (112) face; points experimental, curves predicted using Eqn. 3.

the initial experiment after t = 10 min. When observed under a scanning election microscope (E.T.E.C. Autoscan) and a differential interference contrast microscope (Zeiss Ultraphot 111-M) the original crystal faces showed microcracks, dislocation etch pits and inclusions. The initial surge was probably due to the elimination of the 'disturbed' surface.

Fig. 4 shows K_{obs} [2] plotted as a function of $u^{1/2}$ and includes curves predicted by substituting values of the apparent rate constants for the transport- and surface-controlled reactions, K_t and K_r respectively (see later), into Eqn. 3. The curves are in excellent agreement with the experimental values of K_{obs} at the lower flow rates but diverge at higher flow rates. A change in slope whereby K_{obs} becomes independent of flow rate is usually taken to indicate a change to a surface-controlled reaction (Bircumshaw and Riddiford, 1952). Evidence that the reaction is essentially surface-controlled at the higher flow rates was obtained by increasing the flow rate from 5.8 to 8.1 cm · s^{-1} (37°C) at time t = 40 min. The absence of any change in the rate of movement of the crystal face showed that the reaction was independent of flow rate. Nevertheless, the change in slope is greater than predicted by Eqn. 2 and it is apparent that the mixed-transport surface-controlled dissolution model describes the results at the lower flow rates only. Fig. 5 shows that the break in the K_{obs} versus $u^{1/2}$ curve occurs at a lower flow rate as the

[2] The units of K_{obs} (cm · s^{-1}) are the same as k_{obs} in Eqn. 2, but it should be noted that K_{obs} is an apparent rate constant determined directly at the boundary movement of a crystal face with time, while k_{obs} is a rate constant for the dissolution reaction measured as a concentration change with time.

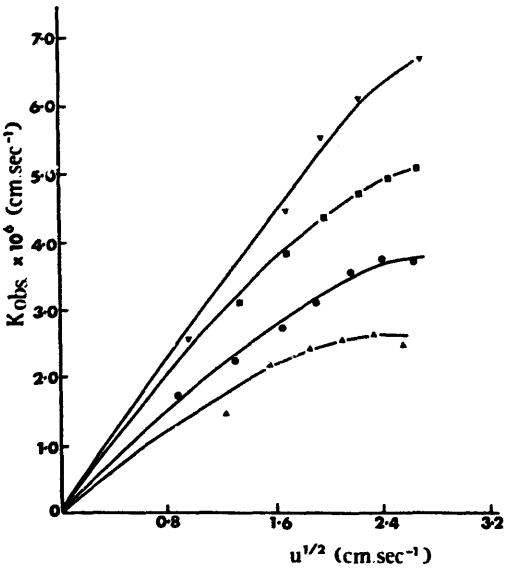

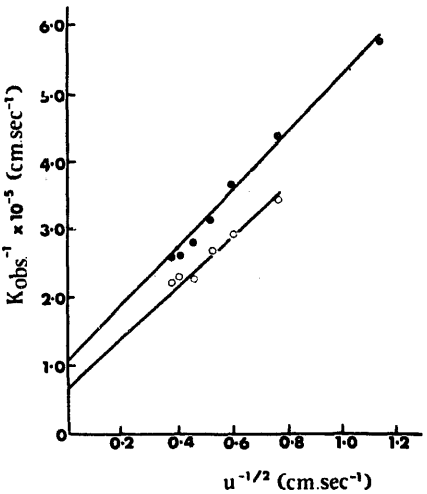

Fig. 5. Dependence of K_{obs} for the (111) face on flow rate: ▲, 30°C; ●, 37°C; ■, 41°C; ▼, 45.5°C.

Fig. 6. Plot of reciprocal of K_{obs} against reciprocal of square root of flow rate for the (111) ● and (112) ○ faces at 37°C. Weighted least squares fitting of the data includes the first 4 data points at the lower flow rates, for each face.

temperature is reduced. Hence the discrepancy between the observed and predicted values of K_{obs} depends on both flow rate and temperature and is not simply an effect of non-laminar flow.

Fig. 4 shows that K_{obs} for the (112) face was greater than for the (111) face at all flow rates studied. Because of differences in the angles at which the faces were presented to the flowing solvent, it was necessary to show that the observed dissolution anisotropy was due to inherent crystalline properties and not to a hydrodynamic effect. This was achieved by angling a crystal on the wire support such that a (111) face occupied the (112) position. Dissolution rates of the (111) face were the same in both positions.

Fig. 6 shows K_{obs}^{-1} versus $u^{-1/2}$ for the (111) and (112) faces plotted according to Eqn. 7. Due to the divergence of K_{obs} at the higher flow rates, these values were not included in the weighted least squares fitting of the data. Errors in K_{obs} (y) depend on the variability of the surfaces of individual crystal faces and observer error, but are independent of $u^{-1/2}$. Hence a mean range, F, was calculated from the range of K_{obs} at each value of $u^{-1/2}$, for a given face and temperature, and was used to calculated a weighting factor $1/\Delta$ where

$$\Delta = 1/(y - \tfrac{1}{2}F) - 1/(y + \tfrac{1}{2}F) \qquad (12)$$

The weighted slopes and intercepts were calculated (Carstensen, 1972) and used to determine K_t and K_r respectively.

For each crystal face it might be expected that K_t, and hence the slopes for the (111)

and (112) faces, would be the same. However, from Eqn. 7 the slope equals $3x^{1/2}D^{-2/3}v^{1/6}$, and although D and v are constants, there is a slight difference in x and x^1 for the (111) and (112) faces respectively (Table 1), and therefore in the values of h (Table 2). The values of h were calculated for each flow rate by substituting the appropriate constants into Eqn. 4, and are comparable to those reported by Fee et al. (1976). Since K_t is inversely proportional to h, at any given flow rate $K_t(111) < K_t(112)$, as shown in Table 2.

The values of K_t increase with increasing flow rate, as expected from Eqn. 5 for a transport-controlled reaction. Although a contributory factor, the difference between K_t for the (111) and (112) faces is too small to cause the dissolution anisotropy shown in Fig. 4.

From Eqn. 3, K_{obs} approaches K_t when K_r approaches infinity. Hence, the intercept on the ordinate of Fig. 6 will approach the origin if dissolution is under pure transport control. The positive intercepts indicate that the dissolution process for both the (111) and (112) faces is under mixed control.

Values of K_r obtained from the intercept are given in Table 2 together with values cal-

TABLE 2

APPARENT RATE CONSTANTS AND FILM THICKNESS

Temper- (°C)	Crystal face	u ($cm \cdot s^{-1}$)	$K_{obs} \times 10^6$ ($cm \cdot s^{-1}$) [a]	$K_t \times 10^6$ ($cm \cdot s^{-1}$)	$K_r \times 10^6$ ($cm \cdot s^{-1}$)	$h \times 10^3$ (cm)
37	(111)	0.75	1.73	2.07	10.6	9.73
		1.70	2.28	3.11	8.52	6.49
		2.73	2.74	3.95	8.97	5.11
		3.66	3.16	4.56	10.3	4.42
			$K_{obs} \pm 0.09$ [b]		9.51 [c]	
37	(112)	1.70	2.90	3.50	16.7	5.96
		2.73	3.41	4.44	14.6	4.70
		3.66	3.70	5.14	13.3	4.06
		4.68	4.34	5.81	17.2	3.59
			$K_{obs} \pm 0.22$ [b]		15.3 [c]	
41	(111)	1.79	3.11	3.82	16.8	6.45
		2.83	3.85	4.79	19.4	5.13
		3.89	4.38	5.62	19.8	4.38
		4.90	4.69	6.31	18.3	3.90
		5.96	4.96	6.96	17.3	3.54
			$K_{obs} \pm 0.16$ [b]		18.3 [c]	
41	(112)	1.79	3.60	4.43	19.1	5.93
		2.83	4.41	5.57	21.1	4.72
		3.89	5.09	6.53	23.1	4.03
		4.90	5.26	7.33	18.6	3.58
			$K_{obs} \pm 0.37$ [b]		20.4 [c]	

[a] Mean of two observations.

[b] $K_{obs} \pm 1/2F$, see text.

[c] K_r obtained from intercept values.

culated from Eqn. 6. The values are greater but are of the same order of magnitude as K_t which supports the suggestion that the overall dissolution reaction is under mixed control even at the lowest flow rates studied. Table 2 shows that K_r is independent of flow rate, as expected for a surface-controlled reaction, and is greater for the (112) face than for the (111) face at both 37 and 41°C indicating that the observed dissolution anisotropy is due mainly to differences in the rate of the surface reaction.

Activation energies for dissolution of the (111) and (112) faces at flow rates of 1.89 and 6.60 cm · s^{-1} obtained from Arrhenius plots, Fig. 7, are given in Table 3. At the lower flow rate, the activation energies for both faces are similar but are slightly higher than the range usually accepted for transport-controlled processes, i.e. 2.8–7.0 kcal · mol^{-1} (11.7–29.3 kJ · mol^{-1}). The results are additional support for the suggestion that dissolution is under mixed control even at low flow rates. At the flow rate of 6.60 cm · s^{-1}, the activation energies are within the accepted limits for a surface-controlled reaction (10–20 kcal · mol^{-1}) but differ for the (111) and (112) faces. It is likely that the observed dissolution anisotropy is due to the difference in magnitude between Ea for the two faces. As the temperature is increased there is a reduction in anisotropy at the higher flow rate. This is less evident at the lower flow rate where dissolution is under mixed control and the contribution of the surface reaction towards K_{obs} is small than in the case of a predominantly surface-controlled process. The point at which the curves at the higher flow rate converge corresponds to a temperature of 49°C. This is close to the temperature of 52–53°C at which tetragonal $NiSO_4$ α $6H_2O$ undergoes a transition to monoclinic $NiSO_4$ β $6H_2O$ (Nicholls, 1973). The significance of this observation is unclear.

The difference in the values of surface free energy of the (111) and (112) faces presumably results from differences in the arrangement and packing density (reticular density) together with the varying energy states of the surface atoms. This is analogous to the situation which exists between polymorphic forms of the same crystalline material. Nogami et al. (1969) used a rotating disc technique to investigate the dissolution kinetics

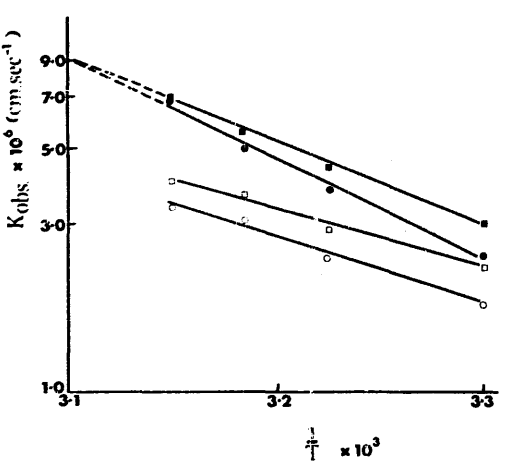

Fig. 7. Arrhenius plots. Flow rates: 1.89 cm · s^{-1}, (111) face ○, (112) face □; 6.60 cm · s^{-1}, (111) face ●, (112) face ■.

TABLE 3

ACTIVATION ENERGIES OF DISSOLUTION FOR THE (111) AND (112) CRYSTAL FACES

u ($cm \cdot s^{-1}$)	E_a ($kcal \cdot mol^{-1}$) [a]	
	(111) face	(112) face
1.89	8.7 (36.4)	7.6 (31.8)
6.60	13.4 (56.1)	10.9 (45.6)

[a] Figures in brackets are Ea values in $kJ \cdot mol^{-1}$.

of barbital polymorphs and treated the data in a manner similar to that given here, except that Eqn. 3 was combined with an equation given by Levich (1962) for the relationship between h and the angular velocity of the rotating disc rather than with Eqn. 4.

Where different faces of the same crystal dissolve at different rates, it seems likely that modification of crystal habit, and the accompanying changes in the relative proportions of the different faces, should have an effect on bulk dissolution rates. The effect of habit modification on the bulk dissolution of crystalline solids is worthy of study.

ACKNOWLEDGEMENTS

The authors thank Dr. R. Phillips and Dr. N. Epstein, Department of Chemical Engineering, University of British Columbia, for the nickel sulfate crystals and Mr. A. Lacis and Mr. P. Musil (Department of Metallurgy) for help with scanning electron microscopy and D.I.C. microscopy.

REFERENCES

Berthoud, A., Theorie de la formation des faces d'un cristal. J. Chem. Phys., 10 (1912) 624–635.

Bircumshaw, L.L. and Riddiford, A.C., Transport control in heterogeneous reactions. Q. Rev. Chem. Soc., 6 (1952) 157–185.

Bunn, C.W., Chemical Crystallography, 2nd. edn. Clarendon Press, Oxford, 1961, p. 2.

Carstensen, J.T., The Theory of Pharmaceutical Systems, Vol. 1. Academic Press, New York, 1972, p. 21.

Carstensen, J.T., Pharmaceutics of Solids and Solid Dosage Forms. J. Wiley and Sons, New York, 1977, p. 74.

Cornell, R.M., Posner, A.M. and Quirk, J.P., Crystal morphology and the dissolution of geothite. J. Inorg. Nucl. Chem., 36 (1974) 1937–1946.

Donbrow, M. and Touitou, E., The dissolution mechanism is a system undergoing complexation: salicylamide in caffeine solution. J. Pharm. Pharmacol., 29 (1977) 524–528.

Fee, J.V., Grant, D.J.W. and Newton, J.M., Effect of solvent flow Reynolds number on dissolution rate of a nondisintegrating solid (potassium chloride). J. Pharm. Sci., 65 (1976) 48–53.

Florence, A.T. and Salole, E.G., Changes in crystallinity and solubility on comminution of digoxin and observations on spironolactone and oestradiol. J. Pharm. Pharmacol., 28 (1976) 637–642.

George, P. and McClure, D.S., Inner orbital splitting. In Cotton, F.A. (Ed.) Progress in Inorganic Chemistry, Vol. 1, Interscience, New York, 1959, p. 458.

Haussuhl, S. und Muller, W., Zur auflowingsgeschwindigkeit von kristallen in wasser. Krist. Tech., 7 (1972) 533–554.

International Critical Tables of Numerical data. Physics, Chemistry and Technology, Vol. 3. McGraw-Hill, New York, 1928, p. 117.

Karshin, V.P. and Grigoryan, V.A., Kinetics of the dissolution of gypsum in water. J. Phys. Chem. U.S.S.R., 44 (1970) 762–763.

King, C.V., Reaction rates at solid–liquid interfaces. J. Am. Chem. Soc., 57 (1935) 828–831.

Lange, N.A. (Ed.), Handbook of Chemistry, 10th edn. McGraw-Hill, New York, 1967, p. 1679.

Levich, V.G., Physicochemical Hydrodynamics. Prentice-Hall, New Jersey, 1962, p. 90.

Milosovich, G., Determination of solubility of a metastable polymorph. J. Pharm. Sci., 53 (1964) 484–487.

Moore, W.J., Physical Chemistry, 4th edn. Prentice-Hall, New Jersey, 1972, p. 438.

Mullin, J.W. and Garside, J., The crystallization of aluminium potassium sulphate: a study in the assessment of crystallizer design data – 1. Singel crystal growth rates. Trans. Inst. Chem. Eng., 45 (1967) T285–T290.

Nicholls, D., Nickel. In Trotman-Dickenson, A.F. (Ed.), Comprehensive Inorganic Chemistry, Vol. 3, Pergamon Press, Oxford, 1973, p. 1131.

Nogami, H., Nagai, T., Fukuoka, E. and Yotsuyanagi, T., Dissolution kinetics of barbital polymorphs. Chem. Pharm. Bull., 17 (1969) 23–31.

Phillips, V.R. and Epstein, N., Growth of nickel sulfate in a laboratory-scale fluidized-bed crystallizer. A.I.Ch.E.J., 20 (1974) 678–687.

Ravdel, A.A. and Moshkevich, A.S., Anisotropy of diffusion-controlled dissolution of a zinc single crystal in mercury. J. Appl. Chem. U.S.S.R., 44 (1971) 328–333.

Roller, P.S., Chemical activity and particle size – II. The rate of solution at slow stirring of anhydrite and gypsum. J. Phys. Chem., 36 (1932) 1202–1231.

Shefter, E. and Higuchi, T., Dissolution behavior of crystalline solvated and nonsolvated forms of some pharmaceuticals. J. Pharm. Sci., 52 (1963) 781–791.

Treivus, E.B., Kinetics of the dissolution of magnesium sulphate heptahydrate single crystals. J. Phys. Chem. U.S.S.R., 38 (1964) 523–525.

Van Name, R.G. and Hill, D.U., On the rates of solution of metals in ferric salts and in chromic acid. Am. J. Sci., 42 (1916) 301–332.

Wurster, D.E. and Taylor, P.W., Dissolution kinetics of certain crystalline forms of prednisolone. J. Pharm. Sci., 54 (1965a) 670–676.

Wurster, D.E. and Taylor, P.W., Dissolution kinetics of certain crystalline forms of prednisolone – II. Influence of low concentrations of sodium lauryl sulfate. J. Pharm. Sci., 54 (1965b) 1654–1658.